Heterogeneous & Homogeneous & Bio- & Nano-
CHEMCATCHEM
CATALYSIS

Supporting Information

Selective One-Pot Two-Step C–C Bond Formation using Metal–Organic Frameworks with Mild Basicity as Heterogeneous Catalysts

Francisco G. Cirujano[+],*[a] Elena López-Maya[+],[b] Marleny Rodríguez-Albelo,[b] Elisa Barea,[b] Jorge A. R. Navarro,*[b] and Dirk E. De Vos*[a]

cctc_201700784_sm_miscellaneous_information.pdf

Contents

I. General methods

All the general reagents and solvents were commercially available and used as received. Thermogravimetric analyses were performed, using a reactive air atmosphere, on a Shimadzu-TGA-50H equipment, at a heating rate of 20 K min^{-1}. XRPD data were obtained on a D2 PHASER Bruker diffractometer using CuKα radiation (λ = 1.5418 Å) by means of a scan in the 2θ range of 5-35° with 0.05°. The compounds were manually grounded in an agate mortar and then deposited in the hollow of a zero-background silicon sample holder. Adsorption isotherms were measured at 77 K for N_2 on a Micromeritics Tristar 3000 volumetric instrument. Prior to measurement, powder samples were heated 7 h at 423 K and outgassed to 10^{-1} Pa. TEM analysis was done using a FEI Talos F200X electron microscope operating at 200 kV. The TEM samples were prepared by suspending 1mg of the powder materials in 1mL of absolute ethanol for 20 minutes to disperse the nanoparticles into the solution and subsequently the materials were hold using a TEM grid (Holey Carbon type) and dipped into the solution for 20 times. Finally they were dried overnight.

The supernatant liquid phase of the catalytic reaction was analyzed by GC/MS using a GC Shimadzu 2014 GC instrument equipped with a FID detector and a CP-Sil 5 CB column. Mass Spectra were obtained with a GC/MS Agilent 6890 gas chromatograph, equipped with a HP-5MS column, coupled to a 5973 MSD mass spectrometer with electron impact ionization. NMR Spectra of the liquid phase was recorded with an AVANCE 400 MHz spectrometer (Bruker, Germany) in $CDCl_3$ at room temperature.

II. Synthesis

Synthesis of $[Ni_8(OH)_4(H_2O)_2$(1,4-bis(1H-pyrazol-4-yl)benzene$)_6]$ (NiBDP), $[Ni_8(OH)_4(H_2O)_2$(2-Hydroxo[1,4-bis(1H-pyrazol-4-yl)benzene]$)_6]$ (NiBDP-OH) and $[Ni_8(OH)_4(H_2O)_2$(2-Amino[1,4-bis(1H-pyrazol-4-yl)benzene]$)_6]$ (NiBDP-NH_2)

The starting ligands were synthesized according to previously reported procedures.[1] The synthesis of MOFs samples **NiBDP**, **NiBDP-OH** and **NiBDP-NH_2**were prepared according to the procedure reported by our group,[2] with subtle changes as follows: in a typical synthesis, 631 mg (3 mmol) of 4,4'-benzene-1,4-diylbis(1H-pyrazole) were dissolved in 160 mL of N,N'-dimethylformamide and 992 mg (4 mmol) of $Ni(CH_3COO)_2 \cdot 4\ H_2O$ were dissolved in 40 mL of H_2O. The two solutions were mixed and refluxed for 12 h under stirring. The solid obtained was filtered off and washed with N,N'-dimethylformamide, ethanol and diethyl ether, yielding the corresponding MOF.

KOH postsynthetic functionalization of NiBDP, NiBDP-OH and NiBDP-NH_2.

The postsynthetical modification of **NiBDP** and **NiBDP-OH** materials were done according to previously reported procedure by our group[3], with activation of as synthesized MOFs thermally at 423 K and outgassed to 10^{-1} Pa for 12 h, in order to obtain solvent-free porous matrix. Afterwards, 0.055 mmol of **NiBDP** and **NiBDP-OH** was suspended in 0.35 M KOH absolute ethanol solution (5.5 mL) and 0.055 mmol of **NiBDP-NH$_2$** activated material was suspended in 18 mL. The resulting suspensions were stirred overnight under an inert N_2 atmosphere, filtered off and washed copiously with absolute ethanol yielding the corresponding compounds $K[Ni_8(OH)_3(C_2H_5O)_3(H_2O)_2(C_{12}H_8N_4)_{5.5}]$ **NiBDP@K,** $K_3[Ni_8(OH)_3(C_2H_5O)(H_2O)_6(C_{12}H_7N_4O)_5]$ **NiBDP-OH@K** and $K[Ni_8(OH)_3(C_2H_5O)_3(H_2O)_2(C_{12}H_9N_5)_{5.5}]$ **NiBDP-NH$_2$@K**.

ICP-MS composition for **NiBDP@K**: Ni, 404.30 ppm; K, 40.02 ppm.
ICP-MS composition for **NiBDP-OH@K:** Ni, 260.70 ppm; K, 64.89 ppm.
ICP-MS composition for **NiBDP-NH$_2$@K**: Ni, 330.30 ppm; K, 30.30 ppm

Preparation of ion exchanged materials $Cu_{0.5}(Ni_5Cu_3(OH)_6(H_2O)_2((1,4\text{-bis}(1H\text{-pyrazol-4-yl})benzene))_{5.5})(Cu(ClO_4)_{1.5})$ [NiBDP@Cu], $Cu_{1.5}(Ni_8(OH)_4(H_2O)_2((2\text{-Hydroxo}[1,4\text{-bis}(1H\text{-pyrazol-4-yl})benzene])_5])(Cu(ClO_4)_2)_{0.5}$ [NiBDP-OH@Cu] and $Cu_{1.5}(Ni_8(OH)_6(H_2O)_2((2\text{-Amino}[1,4\text{-bis}(1H\text{-pyrazol-4-yl})benzene])_{5.5}(Cu(ClO_4)_2)_{1.5}$ [NiBDP-NH$_2$@Cu].

The materials **NiBDP@K**, **NiBDP-OH@K** and **NiBDP-NH$_2$@K** were used as prepared without previous activation as follow, 100 mg of each material was suspended in 12 mL of 0.1 M methanolic solution of $Cu(ClO_4)_2$ with stirring for 16 h at room temperature. The post-modified materials were subsequently filtered off, washed with methanol and dried in air. Afterwards, the solids were suspended in 50 mL of methanol for 2 h in order to remove the eventual absorbed ion pairs. Finally, the suspension was filtered off and washed with methanol to isolate **NiBDP@Cu**, **NiBDP-OH@Cu** or **NiBDP-NH$_2$@Cu**

Anal. calc. for $Cu_{0.5}(Ni_5Cu_3(OH)_6(H_2O)_2(C_{12}H_8N_4)_{5.5})(Cu(ClO_4)_2)_{1.5}(H_2O)_{15}$ **(NiBDP@Cu)**: C, 32.18; H, 3.44; N, 12.51;

Anal. Found: C, 32.14; H, 3.51; N, 12.32.

Calculated residue from TGA for **NiBDP@Cu**: $(NiO)_5(CuO)_5$: 35.3%; Found: 36.1%.

ICP-MS composition for **NiBDP@Cu**: Ni, 94.8ppm; Cu, 98.6ppm; K, 1.32ppm.

Anal. calc. for $Cu_{1.5}(Ni_8(OH)_4(H_2O)_6(C_{12}H_7N_4O)_5)(Cu(ClO_4)_2)_{0.5}(H_2O)_{14}$ **(NiBDP-OH@Cu)**: C, 31.90; H, 3.61; N, 12.40;
Anal. Found: C, 31.68; H, 3.83; N, 12.57.

Calculated residue from TGA for **NiBDP-OH@Cu**: $(NiO)_8(CuO)_2$: 38.9%; Found: 37.1%.

ICP-MS composition for **NiBDP-OH@Cu**: Ni, 35.4ppm; Cu, 8.5ppm; K, 0.7ppm.

Anal. calc. for $Cu_{0.5}(Ni_8(OH)_6(H_2O)_2(C_{12}H_9N_5)_{5.5})(Cu(ClO_4)_2)_{1.5}(H_2O)_{16}$ **(NiBDP-NH_2@Cu)**: C, 30.06; H, 3.50; N, 14.60;
Anal. Found: C, 30.69; H, 3.82; N, 14.37.

Calculated residue from TGA for **NiBDP-NH_2@Cu**: $(NiO)_8(CuO)_2$: 31.3%; Found: 30.6%.

ICP-MS composition for **NiBDP-NH_2@Cu**: Ni, 12.4 ppm; Cu, 3.33 ppm; K, 0.41ppm.

Preparation of material $(Ni_4Cu_4(OH)_4(H_2O)_2((1,4\text{-bis}(1H\text{-pyrazol-}4\text{-yl})benzene))_6)(Cu(ClO_4)_{1.5})$ [NiBDPxCu].

In order to confirm the incorporation of Cu(II) in the cluster, we have carried out a cation exchange of the pristine **NiBDP** with a $Cu(ClO_4)_2$ solution yielding also a material with a high copper content (named as **NiBDPxCu**), as concluded from ICP-MS, energy dispersive X-ray spectroscopy (EDX) and elemental analyses.

The material **NiBDP** was activated thermally at 423 K and outgassed to 10^{-1} Pa for 12h, in order to obtain solvent-free porous matrix. Afterwards, 100 mg of each material was suspended in 12 mL of a 0.1M methanolic solution of the $Cu(ClO_4)_2$ with stirring for 16 h at room temperature. The material obtained was filtered off, washed with methanol and dried in air. Subsequently, the solid was suspended in 50 mL of methanol for 2 h in order to remove the eventual absorbed ion pairs. Finally, the suspension was filtered off and washed with methanol to isolate **NiBDPxCu**.

Anal. calc. for $(Ni_4Cu_4(OH)_4(H_2O)_2(C_{12}H_8N_4)_6)(Cu(ClO_4)_2)_{1.5}(H_2O)_{28}$ **(NiBDPxCu)**: C, 31.55; H, 4.12; N, 12.26;
Anal. Found: C, 30.85; H, 3.99; N, 11.56

Calculated residue from TGA for **NiBDPxCu**: $(NiO)_4(CuO)_{5.5}$: 32.5%; Found: 33.4%.

ICP-MS composition for **NiBDPxCu**: Ni, 8.53 ppm; Cu, 13.62 ppm.

X-ray powder diffraction (XRPD) also proves the maintenance of the characteristic cubic symmetry as found in **NiBDP@Cu** (Figure S2). On the other hand, the presence of $Cu(ClO_4)_2$ ion pairs in the pore voids is responsible for a significant diminution of N_2 adsorption capacity for **NiBDPxCu** and **NiBDP@Cu** materials. Moreover the occurrence of $Cu(ClO_4)_2$ is also confirmed by infrared spectra with several characteristic features in the 1100 cm^{-1} region (Figure S3-S4)

Table S1. Amount of K and Cu with respect to Ni in the MOFs

MOF	*K/Ni*	*Cu/Ni*
NiBDP@K	0.10	-
NiBDP_OH@K	0.25	-
NiBDP_NH_2@K	0.10	-
NiBDP@Cu	0.01	1.04
NiBDP_OH@Cu	0.02	0.24
NiBDP_NH_2@Cu	0.03	0.27

III. MOF characterization

❖ Powder X-Ray Diffraction

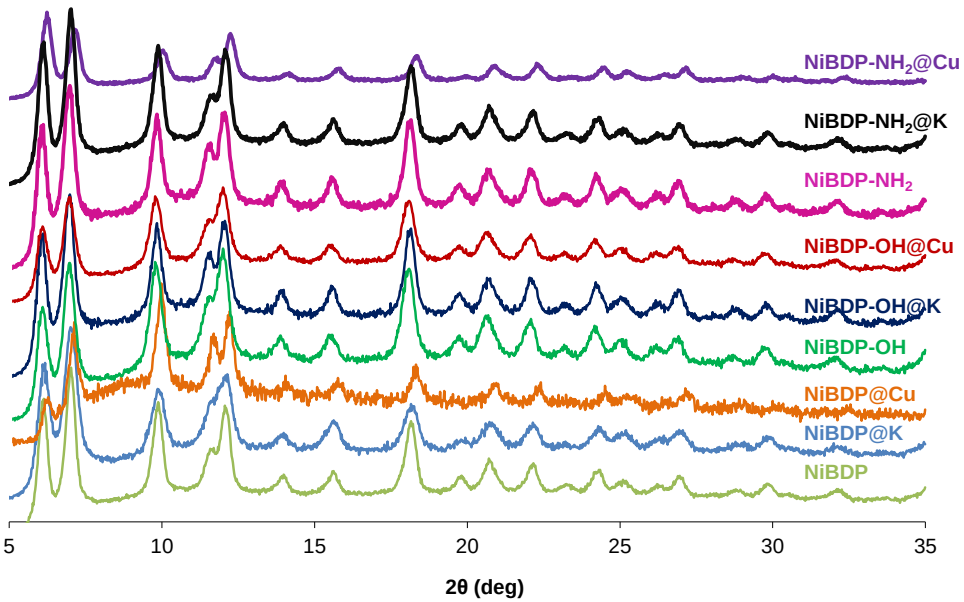

Figure S1. PXRD of samples **NiBDP**, **NiBDP@K, NiBDP@Cu, NiBDP-OH, NiBDP-OH@K, NiBDP-OH@Cu, NiBDP-NH_2, NiBDP-NH_2@K** and **NiBDP-NH_2@Cu.**

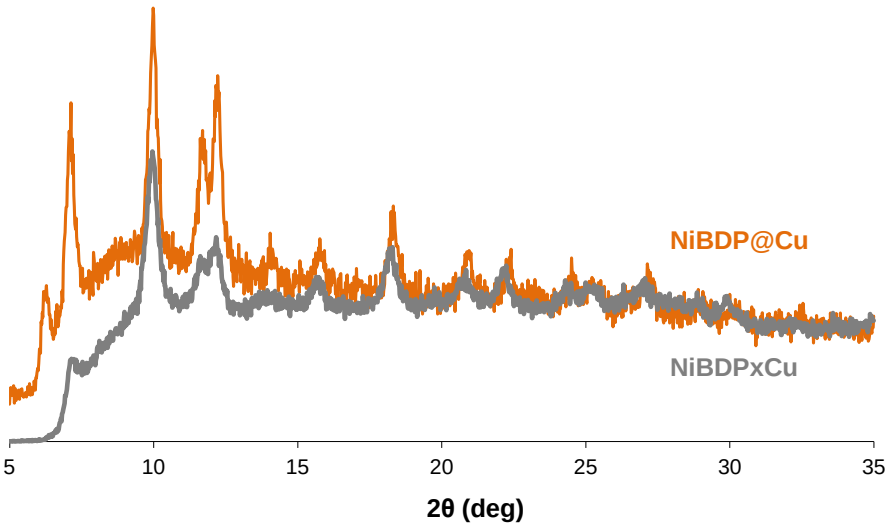

Figure S2. Comparison of PXRD patterns of samples **NiBDP@Cu** and **NiBDPxCu.**

❖ FTIR Spectra

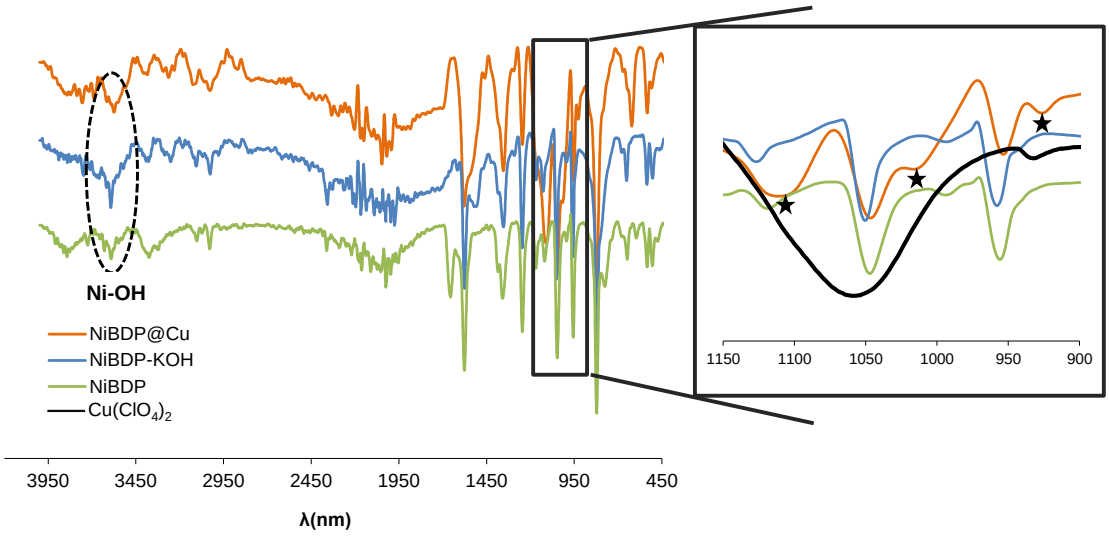

Figure S3. FTIR spectra for **NiBDP**, **NiBDP@K** , **NiBDP@Cu** and $Cu(ClO_4)_2$.

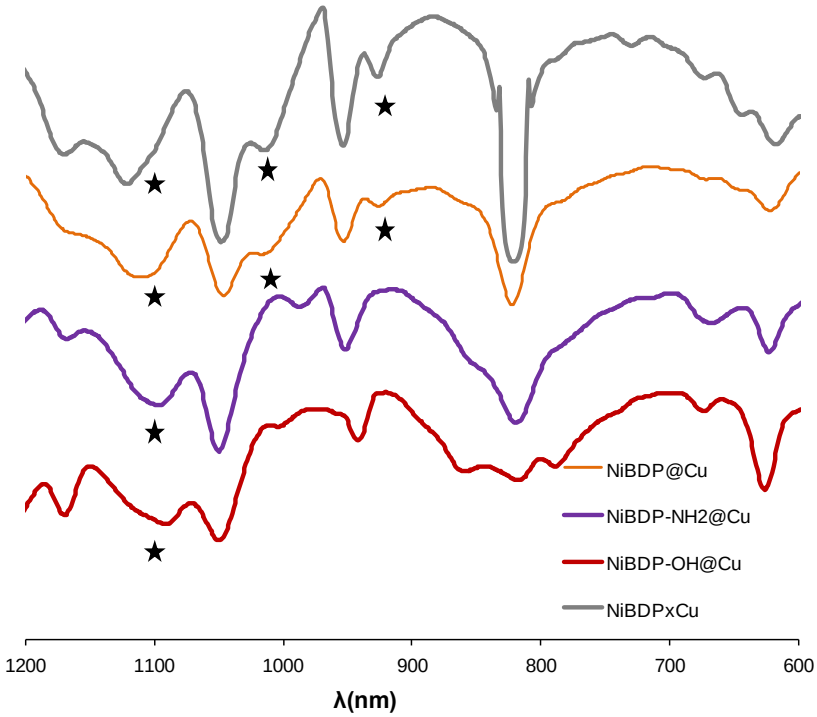

Figure S4. FTIR spectra for **NiBDP@Cu, NiBDPxCu, NiBDP-OH@Cu** and **NiBDP-NH_2@Cu.**

❖ **Thermal Analysis**

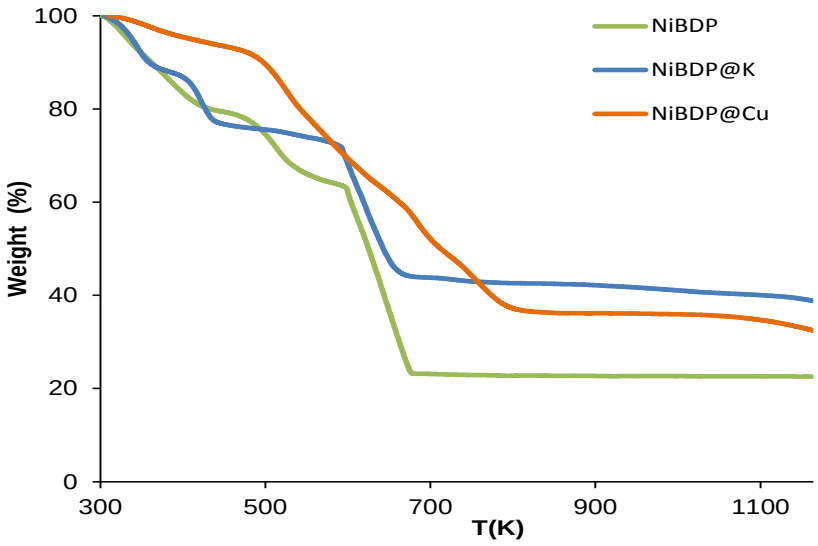

Figure S5. TGA traces for **NiBDP, NiBDP@K** and **NiBDP@Cu** species**.**

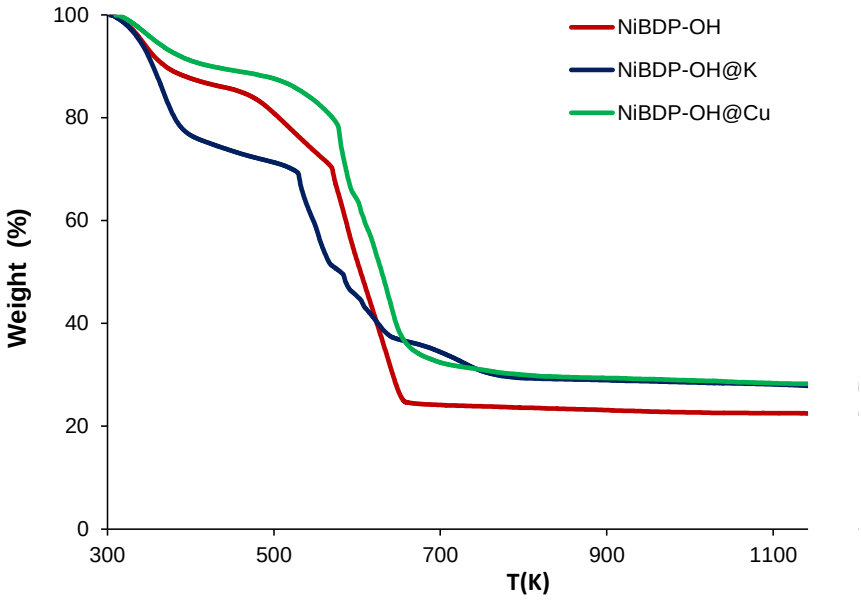

Figure S6. TGA trace for species **NiBDP-OH, NiBDP-OH@K** and **NiBDP-OH@Cu.**

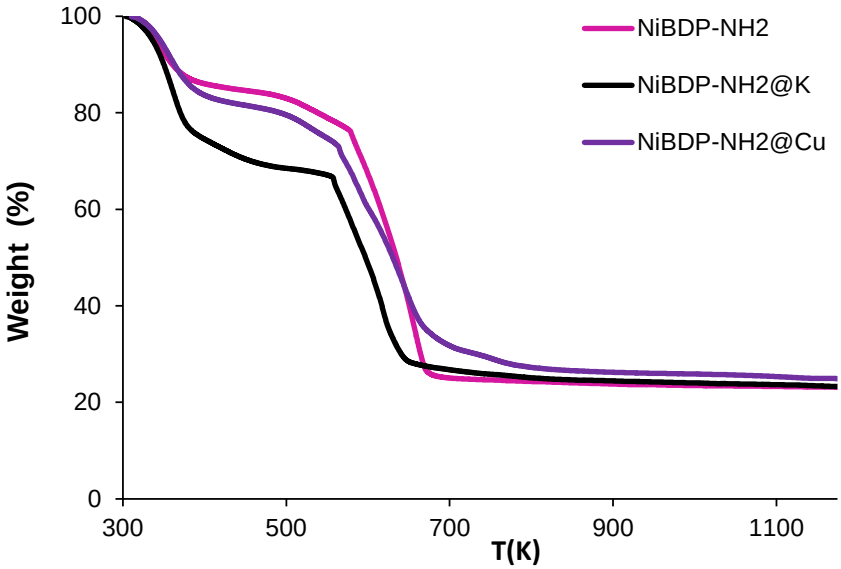

Figure S7. TGA trace for species **NiBDP-NH_2, NiBDP-NH_2@K** and **NiBDP-NH_2@Cu.**

❖ **Transmission Electron Microscopy**

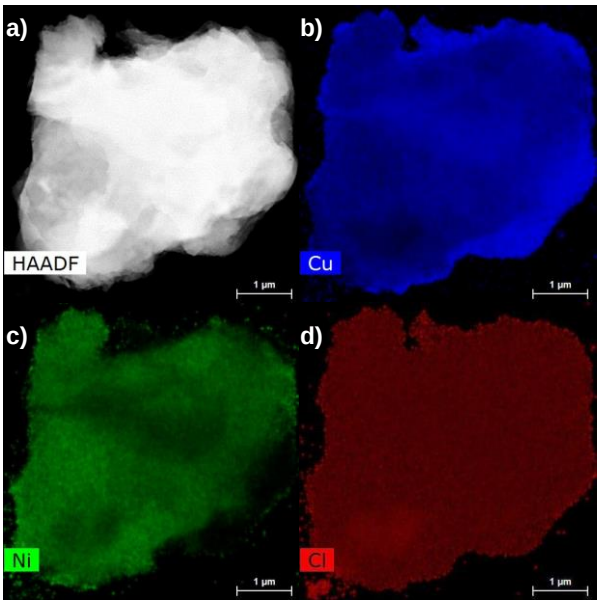

Figure S8. High Resolution Transmission Electron Microscopy (HRTEM) imaging of sample **NiBDP@Cu**. a) In the high angle annular dark-field (HAADF)-TEM images; b) energy-dispersive X-ray spectroscopy (EDX) mapping for Cu element; c) for Cl element; d) for Ni element and d) for Cl element.

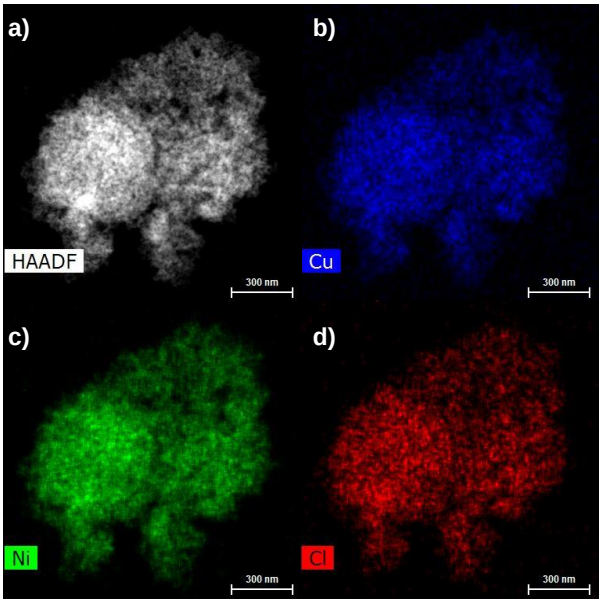

Figure S9. HRTEM imaging of sample **NiBDP-OH@Cu**. a) HAADF-TEM images; b) EDX mapping for Cu element; c) for Cl element; d) for Ni element and d) for Cl element.

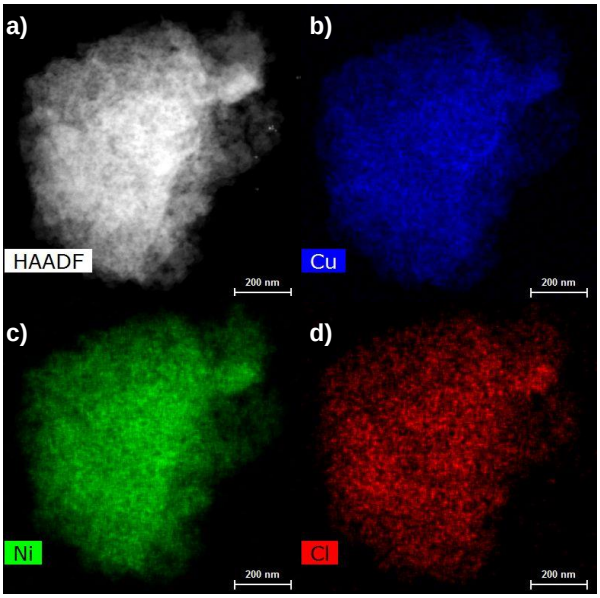

Figure S10. HRTEM imaging of sample **NiBDP-NH$_2$@Cu**. a) HAADF-TEM images; b) EDX mapping for Cu element; c) for Cl element; d) for Ni element and d) for Cl element.

❖ Nitrogen adsorption measurements

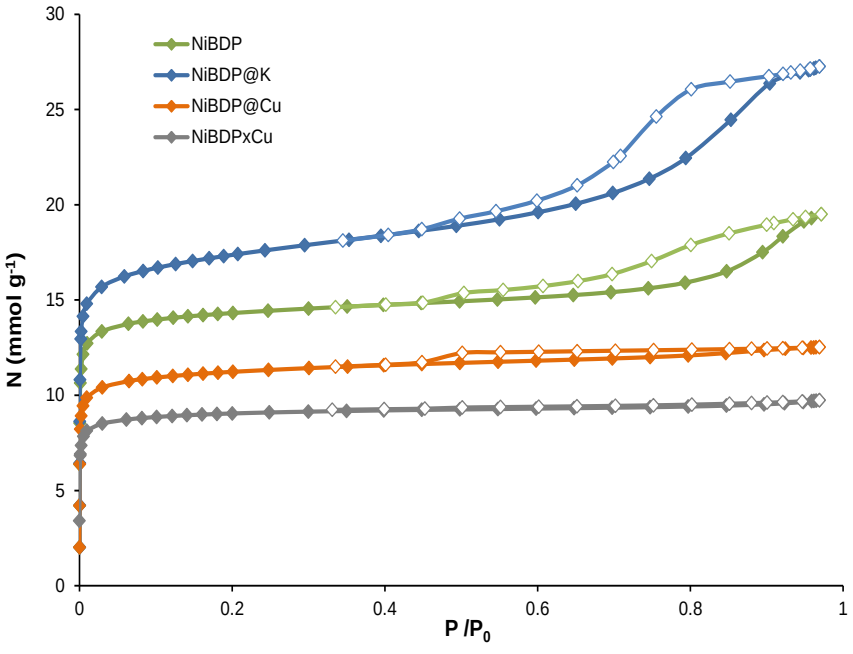

Figure S11. N_2 adsorption isotherms at 77 K for **NiBDP, NiBDPxCu, NiBDP@K** and **NiBDP@Cu**.

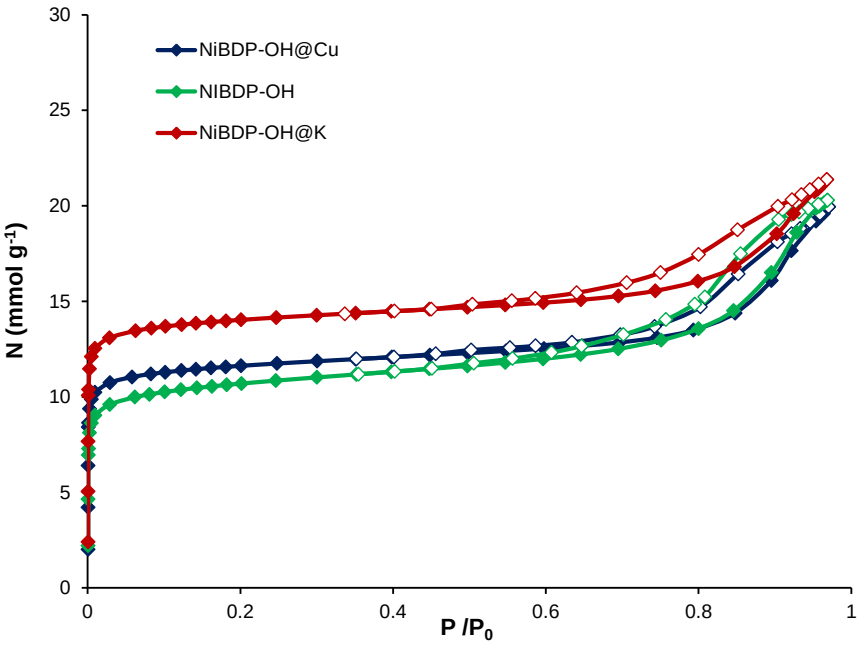

Figure S12. N_2 adsorption isotherms at 77 K for **NiBDP-OH**, **NiBDP-OH@K** and **NiBDP-OH@Cu**.

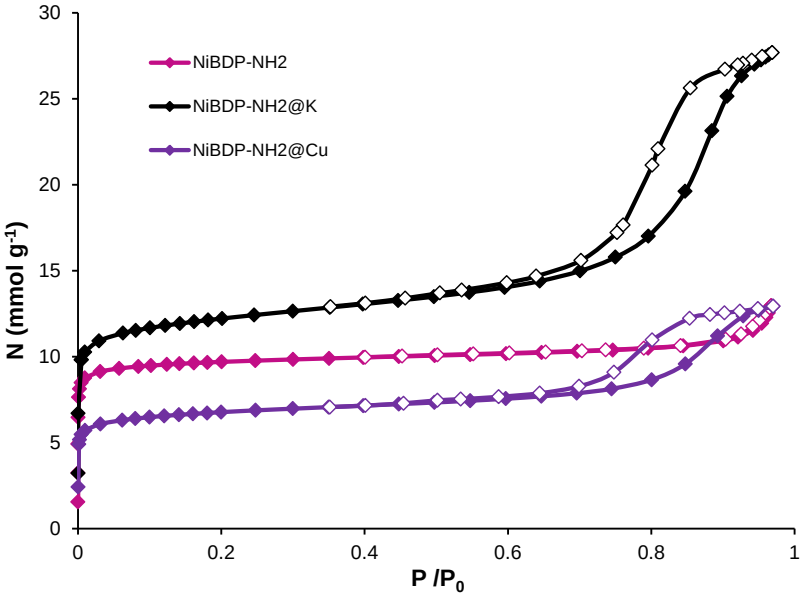

Figure S13. N_2 adsorption isotherms at 77 K for **NiBDP-NH_2**, **NiBDP-NH_2@K** and **NiBDP-NH_2@Cu**.

❖ **Electronic spectra**

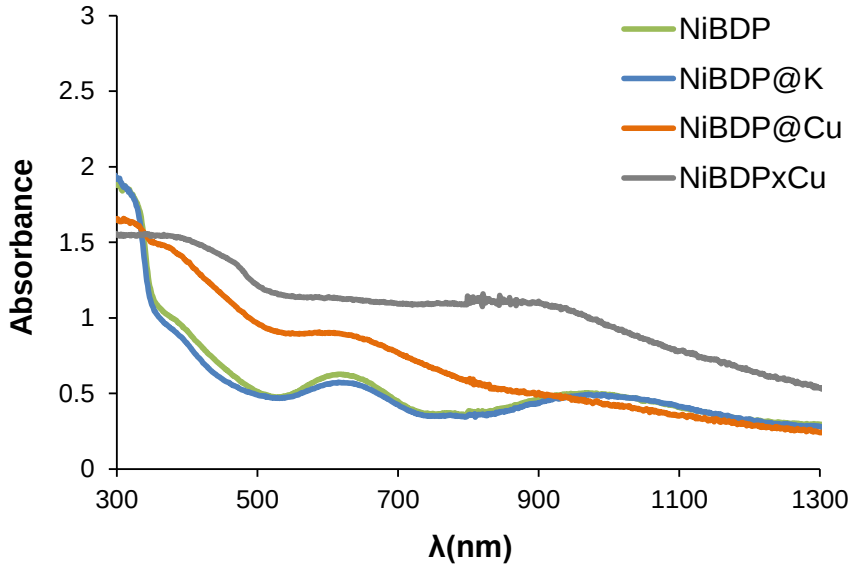

Figure S14. UV-Vis absorption spectra for **NiBDP**, **NiBDP@K** , **NiBDP@Cu**, and **NiBDPxCu**.

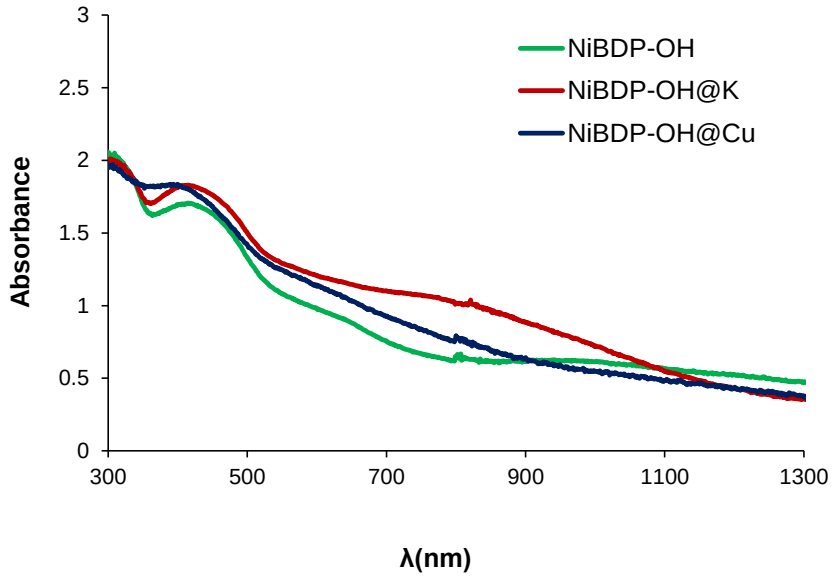

Figure S15. UV-Vis absorption spectra for **NiBDP-OH**, **NiBDP-OH@K** and **NiBDP-OH@Cu**.

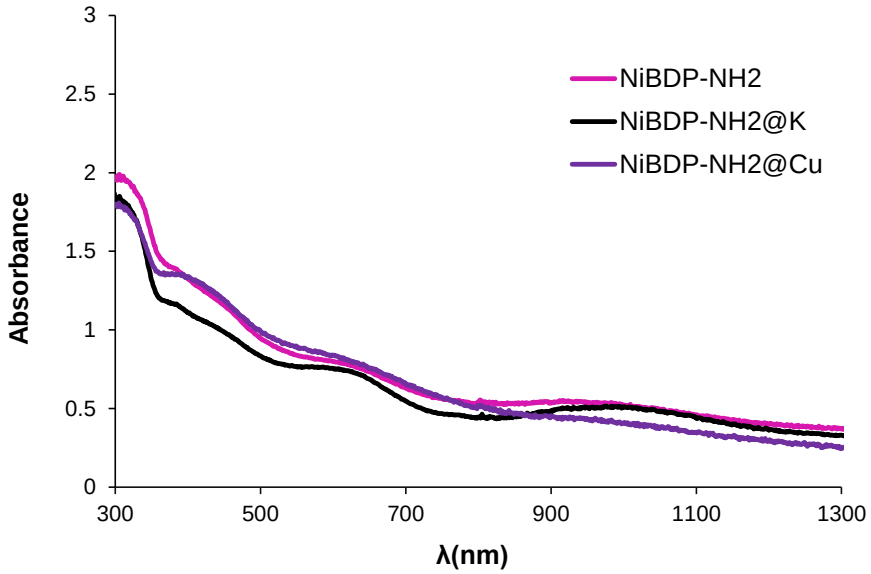

Figure S16. UV-Vis absorption spectra for **NiBDP-NH$_2$**, **NiBDP-NH$_2$@K** and **NiBDP-NH$_2$@Cu**.

a)

Compounds	Raman Shift (cm^{-1})
Cu_2O	146
CuO	297, 610
NiBDP	958
NiBDP@Cu	959, 354, 299

b)

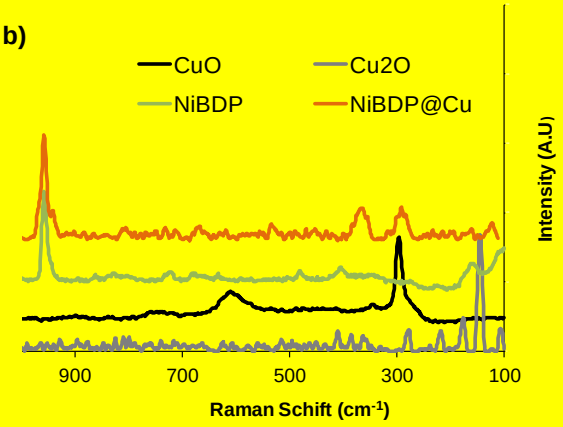

Figure S17.a) Observed Raman Shifts in Cu_2O, CuO, **NiBDP** and **NiBDP@Cu**, b) Raman spectra for Cu_2O, CuO, **NiBDP** and **NiBDP@Cu**.[5]

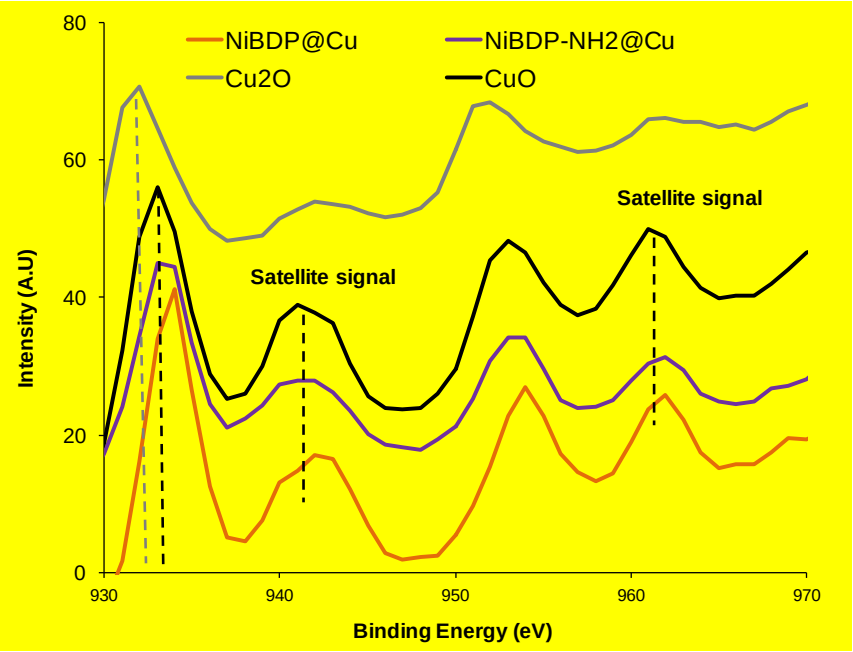

Figure S18. XPS spectra for Cu_2O, CuO, **NiBDP_NH_2@Cu** and **NiBDP@Cu**.

IV. Catalytic reactions

❖ Henry reaction

Nitromethane (53 µl, 1 mmol), benzaldehyde (10 µl, 0.1 mmol) and 2-butanol (0.5 ml) were added to the MOF catalyst (10 mg). Decane (10 µl) was added as an internal standard. The reaction mixture was stirred in a round bottom flask for 48 h under reflux, while the consumption of the starting material was monitored by GC-FID (Gas Chromatography-Flame Ionization Detector). Identification of the reaction products was achieved by comparing the retention times in GC-FID with commercial products but also by H-NMR and GC-MS analysis.

For the recycling test, the used catalyst was isolated from the reaction mixture by centrifugation (3000 rpm, 10 min) and washed with 2-butanol (2 x 3 ml) until the supernatant was the pure solvent, as confirmed by GC-FID. The recovered catalyst was dried and reused under the same reaction conditions. For the hot filtration test, the used catalyst was isolated from the reaction mixture by centrifugation (3000 rpm, 10 min) and the reaction was followed without the catalyst under the same conditions.

❖ **Michael type additions**

Indole (12 mg, 0.1 mmol) or dimethylmalonate (13 mg, 0.1 mmol) where added to the reaction after 48 h and stirred for additional 12 h under reflux to obtain **2** or **3**. The consumption of the starting material was monitored by GC-FID. Identification of the reaction products was achieved by comparing the retention times in GC-FID with commercial products but also by H-NMR and GC-MS analysis.

Table S2. First and second step reactions of Scheme 1 to generate products **1**, **2** and **3** using different Ni and Cu containing catalysts.

	Catalyst	Yield to **1** (%)[a]	r_0 (µmol/ h^{-1})[b]	Yield to **2** (%)[c]	r_0 (µmol/ h^{-1})	Yield to **3** (%)[d]	r_0 (µmol/ h^{-1})
1	**NiBDP**	36	1.6	64	12.4	66	16
2	**NiBDP@K**	51	2	99	19.2	91	40
3	**NiBDP@Cu**	76	3.2	78	14.4	97	48
5	**NiBDP_OH**	64	3.6	99	33.6	99	51
6	**NiBDP_OH@K**	20	2.8	96	42.4	96	38

7	**NiBDP_OH@Cu**	36	2.4	99	25.2	99	42
8	**NiBDP_NH_2**	41	4.4	93	33.6	99	70
9	**NiBDP_NH_2@K**	20	3.6	96	38	96	40
10	**NiBDP_NH_2@Cu**	50	2.8	99	33.6	99	53
11	$Cu(ClO_4)_2$	27	0.5	n.d.	-	n.d.	-
12	$Ni(OAc)_2$	48	1.7	99	17.6	32	9.1
13	$Ni(OAc)_2$+ $Cu(ClO_4)_2$	67	0.7	99	8.4	22	0.4
14	$Ni(py)_2$	68	2.8	-	-	61	21
15	$Ni(OH)_2$	29	1.2	-	-	91	17
16	$Ni_2(dhtp)(H_2O)_2 \cdot 8H_2O$	8	0.2	-	-	37	6
17	$Cu(py)_2$	20	0.8	-	-	77	32
18	$Cu(OH)_2$	38	0.8	-	-	82	13
19	$Cu_3(btc)_2$	7	0.2	-	-	67	7

[a]0.1 mmol of benzaldehyde, 1 mmol nitromethane, 10 mg catalyst (~40%mol of NiO and CuO sites in the MOF with respect to the substrate), 0.5 ml 2-propanol, reflux, 48 h. [b]mol of product obtained divided by time (for conversions < 30%). [c]0.1 mmol of β-nitrostyrene, 0.1 mmol dimethylmalonate, 10 mg catalyst, 0.5 ml 2-propanol, reflux, 24 h. [d]0.1 mmol of β-nitrostyrene, 0.1 mmol indole, 10 mg catalyst, 0.5 ml 2-propanol, reflux, 12 h.

Table S3. Conversions and selectivity after 48 h of reaction time for the Henry reaction between benzaldehyde and nitromethane using **NiBDP@Cu** as catalyst.[a]

Conversion (%)			Selectivity (%)		
1st use	2nd use	3rd use	1st use	2nd use	3rd use
81	76	63	94	92	93

[a] the catalyst was separated by centrifugation, washed with 2-butanol (1 ml), isolated by centrifugation and dried under vacuum before the reuse.

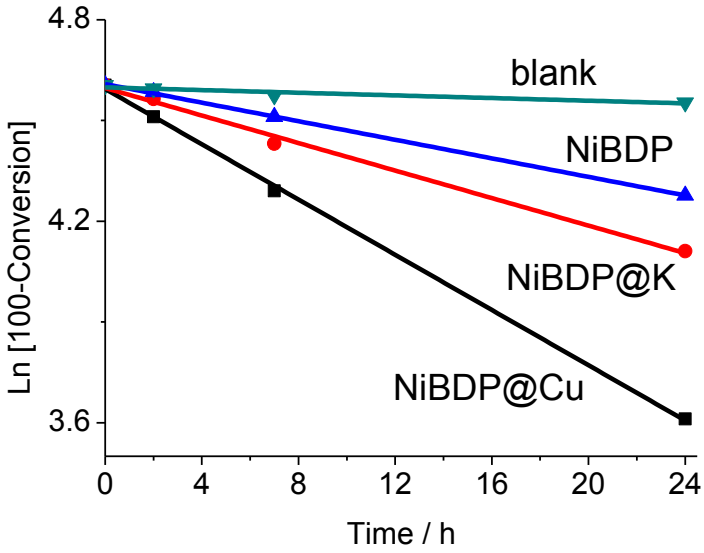

Figure S19. Calculation of the pseudo-first order kinetic rate constant, k, from the slope of the ln[100-(Nitrosyterene yield)] vs time plot using as catalysts: a) **NiBDP@Cu**, b) **NiBDP@K**, c) **NiBDP**, d) blank.

The kinetic equations from which the kinetic rate constant k (slope) was obtained, together with the quality of the linear fit by means of the correlation coefficient R^2 are shown below for the different tested **NiBDP** MOF catalysts:

A) ln[100-conversion] = - 0.041 · time + 4.59 ; R^2 = 0.99
B) ln[100-conversion] = - 0.021 · time + 4.60 ; R^2 = 0.99
C) ln[100-conversion] = - 0.014 · time + 4.61 ; R^2 = 0.99
D) ln[100-conversion] = - 0.001 · time + 4.60 ; R^2 = 0.86

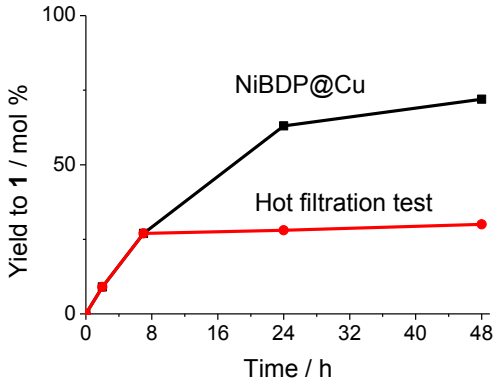

Figure S20. Hot filtration test and reuse of the **NiBDP@Cu** MOF in the Henry reaction of nitromethane with benzaldehyde

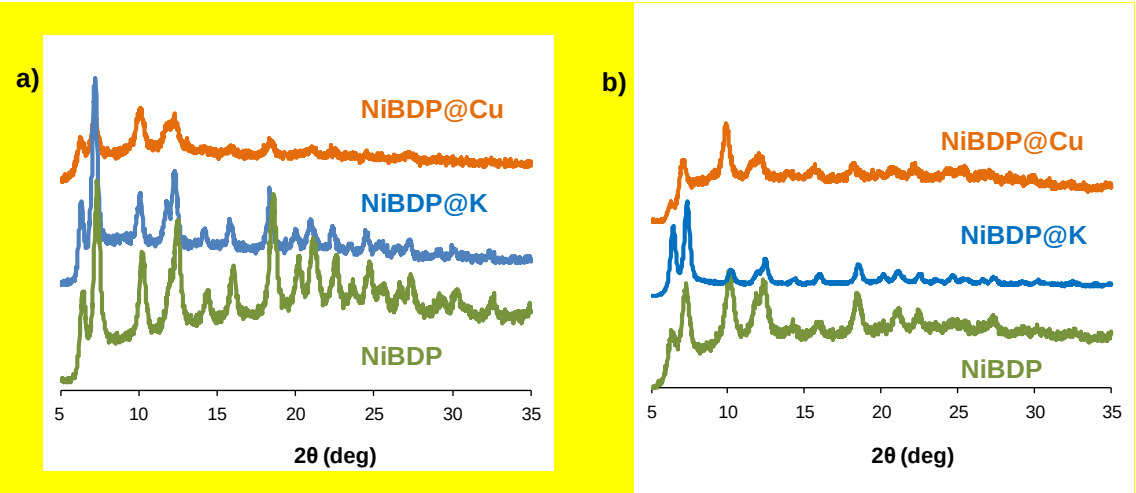

Figure S21. a) XRD of the MOF catalysts after the one-pot two step synthesis of **2** and b) after the one-pot two step synthesis of **3**.

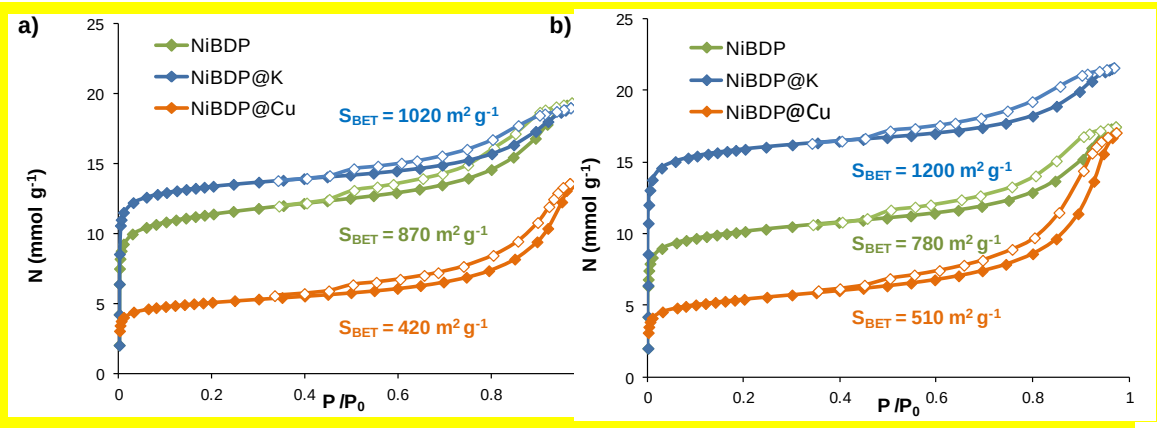

Figure S22. N_2 adsorption isotherms at 77 K for **NiBDP, NiBDP@K** and **NiBDP@Cu a)** after the one-pot two step synthesis of **2** and b) after the one-pot two step synthesis of **3**.

Table S4. BET surface area (m^2g^{-1}) of the catalysts before and after the reaction

Sample	Fresh material	After synthesis of **2**	After synthesis of **3**
NiBDP	1100	870	780
NiBDP@K	1340	1020	1200
NiBDP@Cu	830	420	510

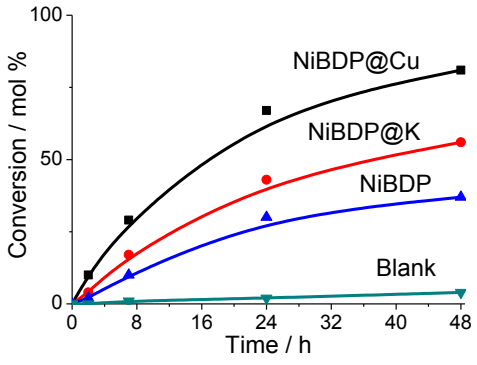

(a)

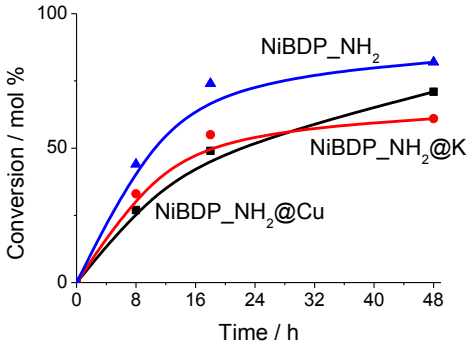

(b)

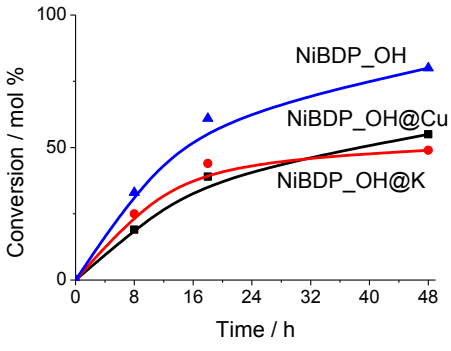

(c)

Figure S23. Kinetic plot (benzaldehyde conversion vs time) for the reaction between nitromethane and benzaldehyde using the **NiBDP** (a), **NiBDP_NH2** (b), **NiBDP_OH** (c) family of metal-organic frameworks.

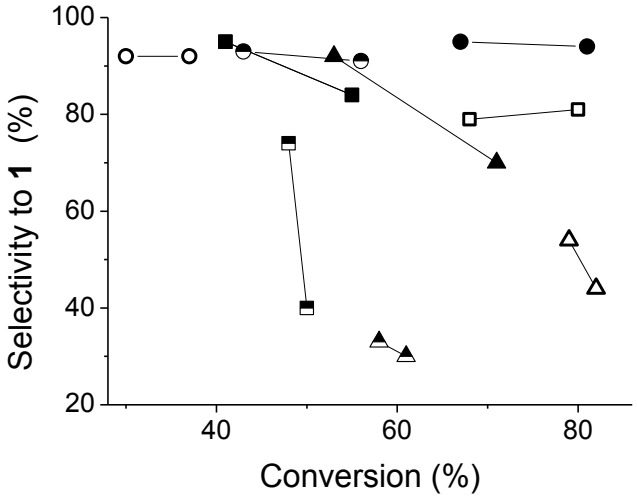

Figure S24. Selectivity to **1** vs. the conversion of benzaldehyde in the Henry reaction using the **NiBDP_X@M** materials, X= H (circle), OH (square), NH_2 (triangle), M= no exchanged metal (empty circle), K (half empty), Cu (full).

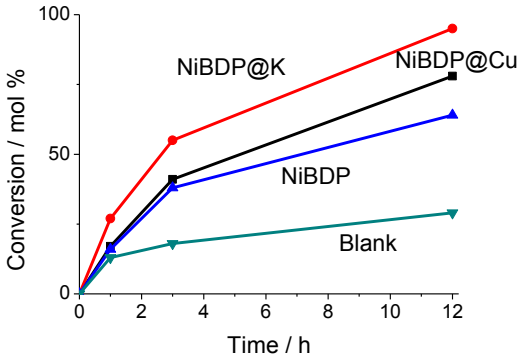

(a)

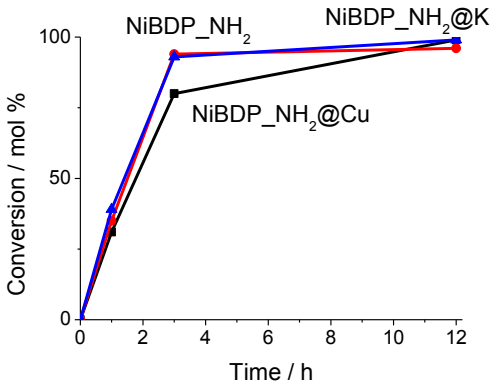

(b)

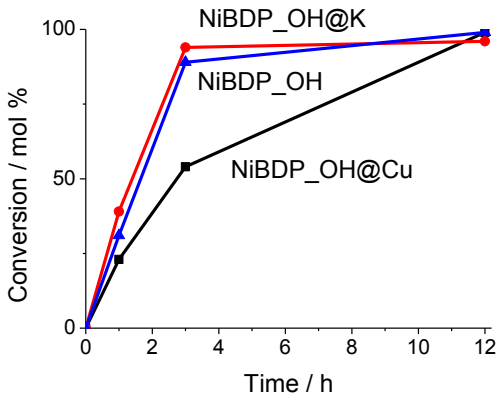

(c)

Figure S25. Kinetic plot (β-nitrostyrene conversion vs time) for the reaction between β-nitrostyrene and dimethylmalonate using the **NiBDP_X** (blue curve), **NiBDP_X@K** (red curve), **NiBDP_X@Cu** (black curve) as heterogeneous catalyst. X = H, NH_2, OH.

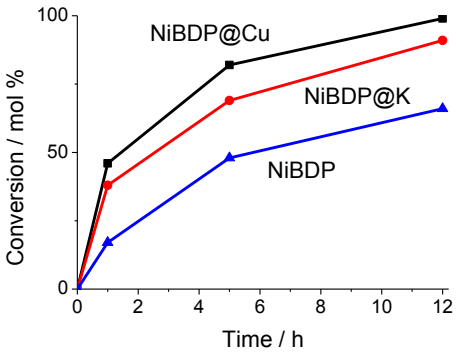

(a)

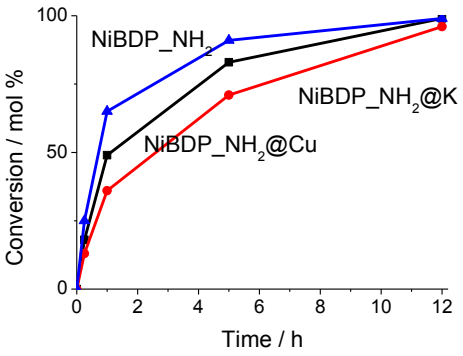

(b)

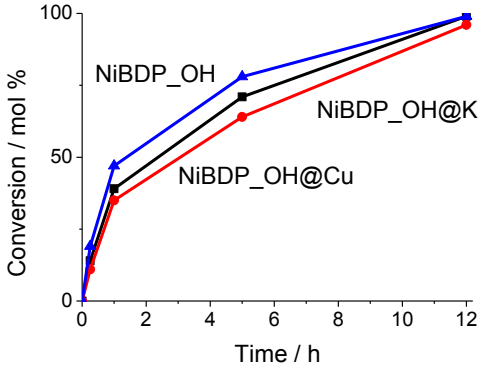

(c)

Figure S26. Kinetic plot (β-nitrostyrene conversion vs time) for the reaction between β-nitrostyrene and indole in 2-butanol using the **NiBDP_X** (blue curve), **NiBDP_X@K** (red curve), **NiBDP_X@Cu** (black curve) as heterogeneous catalyst. X = H, NH_2, OH.

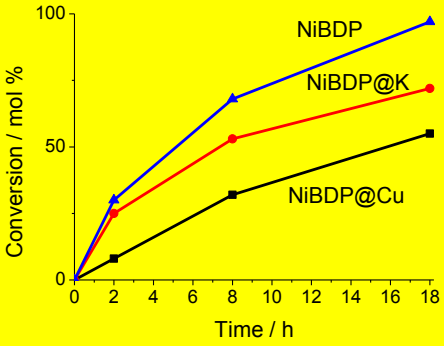

(a)

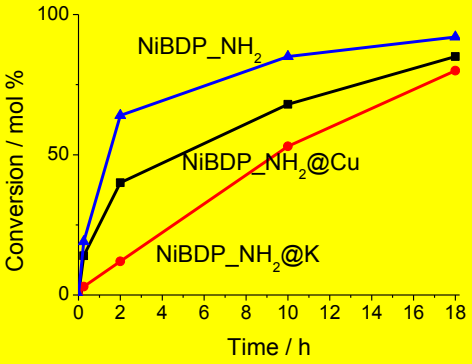

(b)

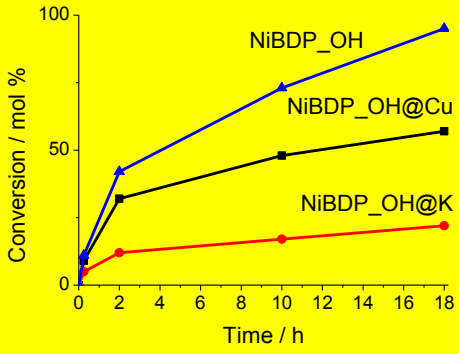

(c)

Figure S27. Kinetic plot (β-nitrostyrene conversion vs time) for the reaction between β-nitrostyrene and indole in toluene using the **NiBDP_X** (blue curve), **NiBDP_X@K** (red curve), **NiBDP_X@Cu** (black curve) as heterogeneous catalyst. X = H, NH_2, OH.

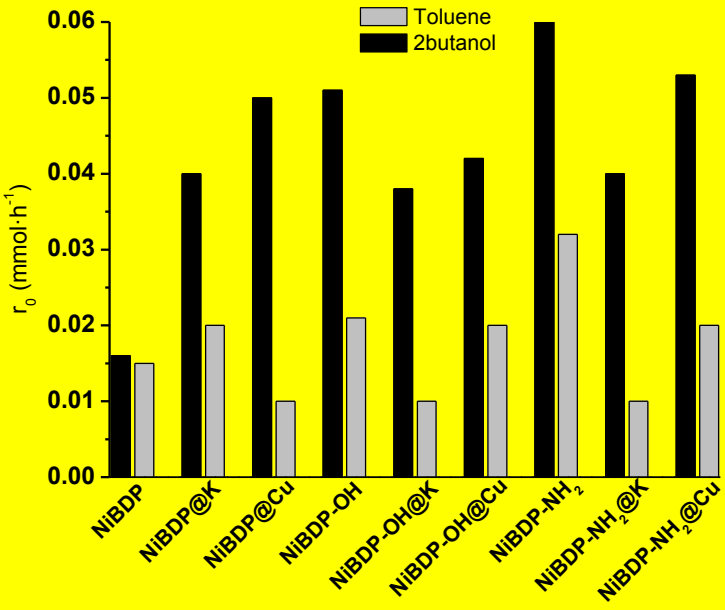

Figure S28. Initial rate for the reaction between β-nitrostyrene (0.1mmol) and indole (0.1mmol) in 2-butanol or toluene (0.5ml) at 100ºC using 10 mg of MOF as heterogeneous catalyst.

Other solids employed as catalysts for comparison with MOFs

Both the Henry reaction and the one-pot synthesis of the substituted indole **3** were performed using of other solid catalysts in order to establish a fair comparison between the MOFs presented in this work and similar Ni or Cu containing solids. The reaction conditions were the same in all cases: 0.1 mmol substrate, 10mg catalyst, 100ºC, 0.5ml 2-butanol.

$Cu(py)_2$

The bispyrazolato-copper(II), $Cu(py)_2$, was prepared according to the procedure reported by Cingolani et al.[5] Briefly, 70mg of pyrazole (Hpz) in 0.5ml were added to 100mg of $Cu(OAc)_2 \cdot H_2O$ in 10ml CH_3CN and stirring at room temperature for 0.5h. The pink solid formed was washed with CH_3CN and dry under nitrogen.

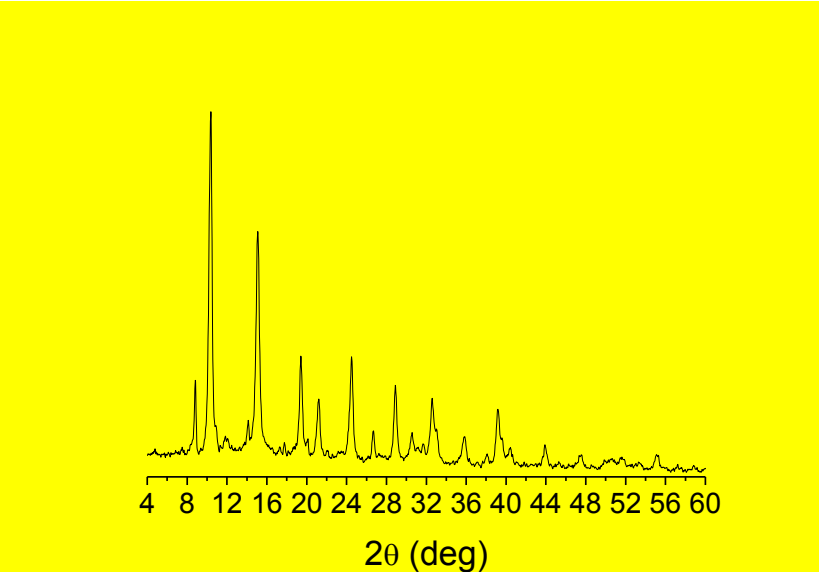

Figure S29. XRD pattern of $Cu(py)_2$

$Cu(OH)_2$

The copper hydroxide was purchased from Sigma-Aldrich.

$Cu_2(btc)_3$

The copper benzene-1,3,5-tricarboxylate (Basolite® C 300) was purchased from Sigma-Aldrich.

$Ni(py)_2$

The bispyrazolato-nickel(II), $ni(py)_2$, was prepared according to the procedure reported by Masciocchi et al.[6] Briefly, 435 mg of pyrazole (Hpz) were added to 400mg of $Ni(OAc)_2 \cdot 4H_2O$ in 12ml of butanol and heated at 130ºC for 4h. The yellow solid formed was washed with butanol and EtOH and dry under nitrogen.

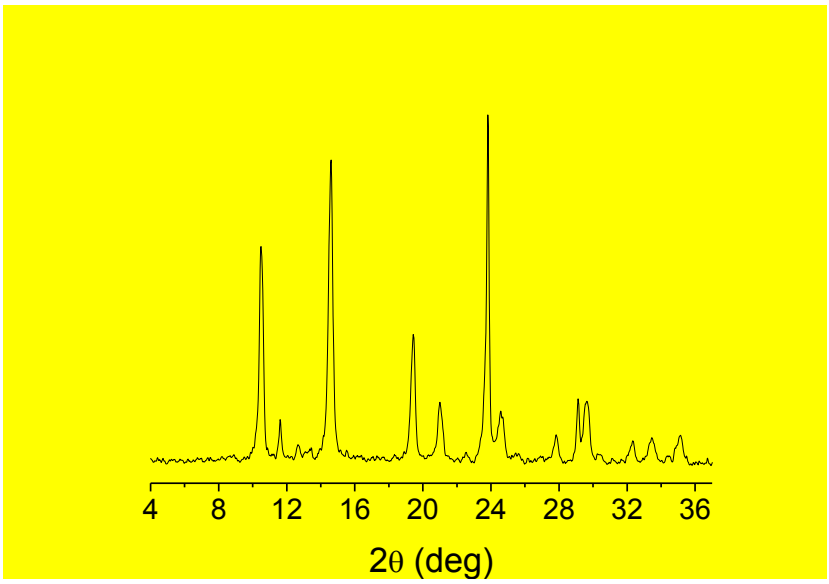

Figure S30. XRD pattern of $Ni(py)_2$

$Ni(OH)_2$

The nickel hydroxide was adapted from a procedure already reported.[7] Briefly, 90 mg of $Ni(OAc)_2 \cdot 4H_2O$ in 2ml of ethylene glycol were dissolved by stirring 0.5h at 120ºC. Then, 100mg of Na_2CO_3 in 5 ml of water were added slowly under stirring at 120ºC and the gel was aged for 1h at that temperature. After centrifugation, the green solid was washed with water and dry at 100ºC overnight.

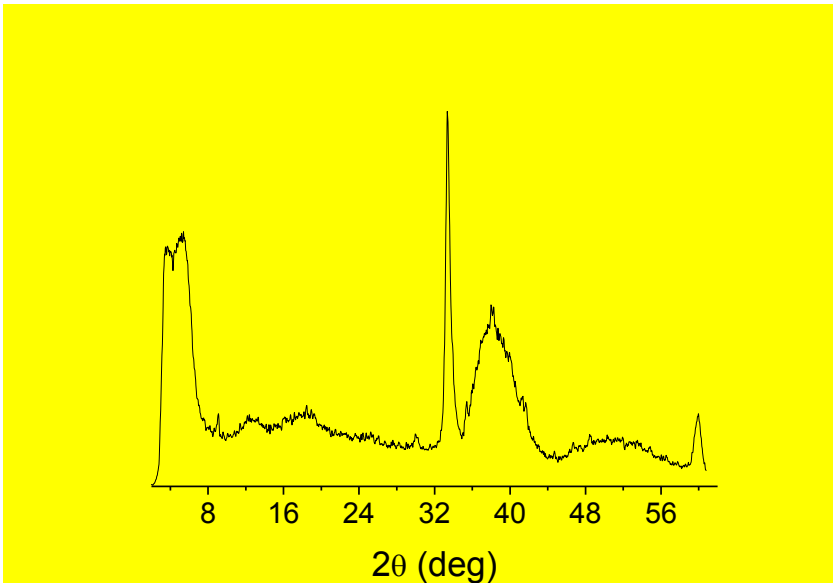

Figure S31. XRD pattern of $Ni(OH)_2$

$Ni_2(dhtp)(H_2O)_2 \cdot 8H_2O$

The Ni-CPO-27 was prepared according to a reported procedure.[8] Briefly, 187mg of $Ni(OAc)_2 \cdot 4H_2O$ in 5ml of water and 75mg of 2,5-dihydroxyterephtalic acid (dhtp) in 5ml THF were mixed, dissolved and heated at 110ºC for three days. The yellow-green powder was washed with water and dry under vacuum.

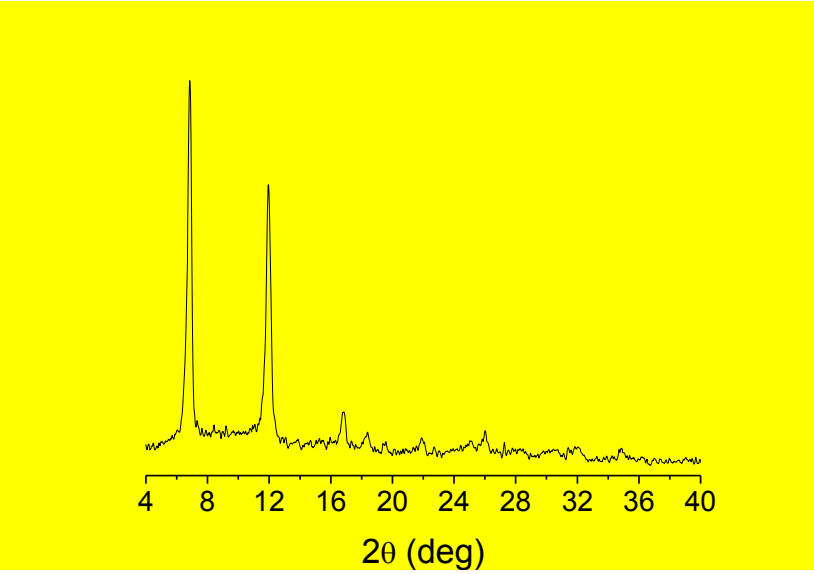

Figure S32. XRD pattern of Ni-CPO-27

V. Characterization of the reaction products

❖ Nitrostyrene (**1**)

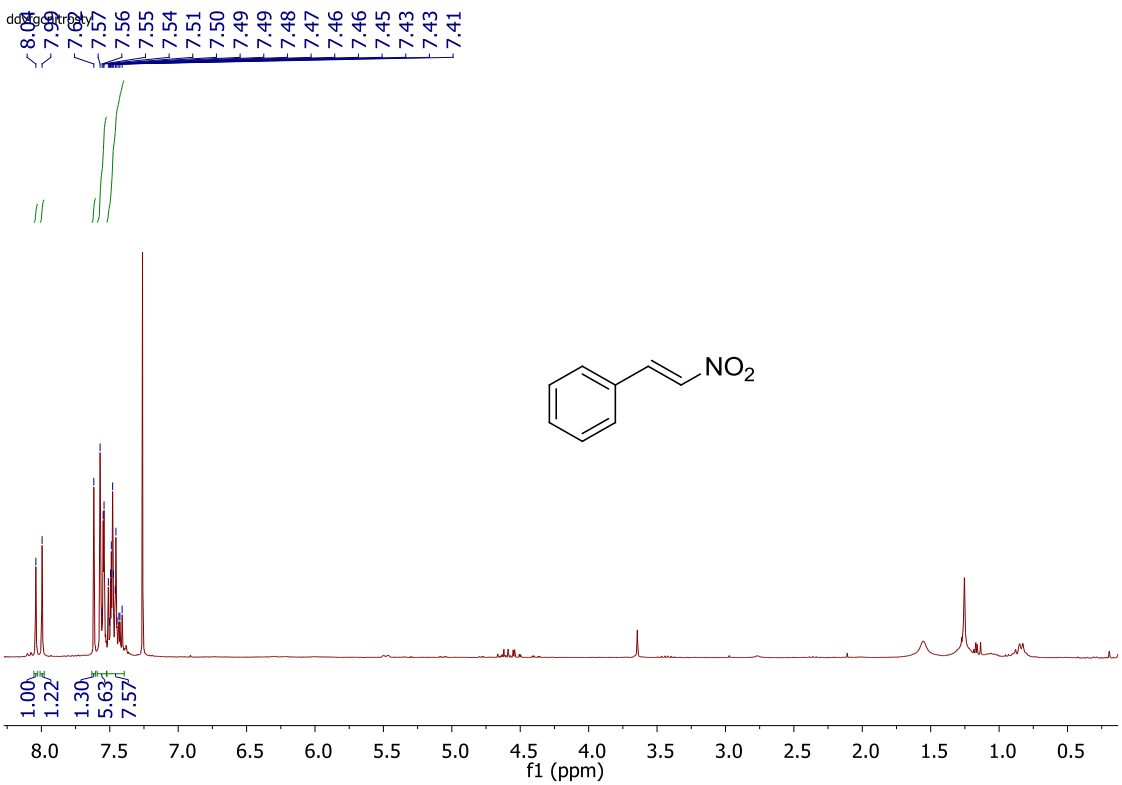

^{1}H NMR (300 MHz, $CDCl_3$) δ 8.04 (s, 1H), 7.99 (s, 1H), 7.59 – 7.53 (m, 5H). The rest of the signal at 7.3-7.7 corresponds to benzaldehyde starting product.

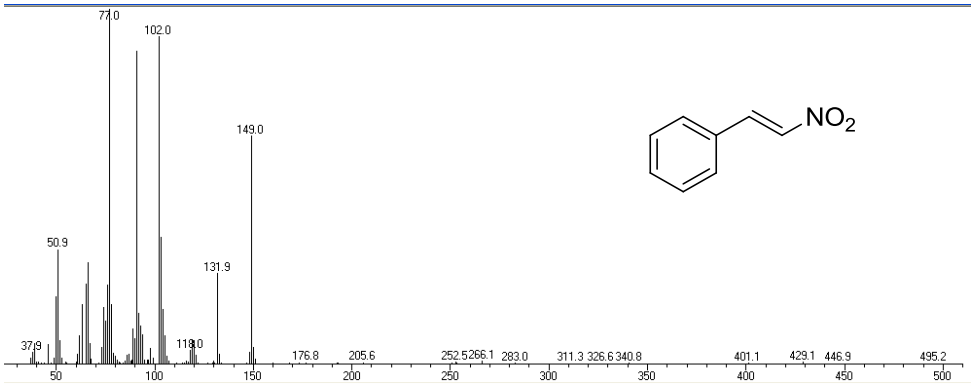

m/z calculated for $C_8H_7NO_2^{+\bullet}$ [$M^{+\bullet}$]: 149

❖ (1,3-dinitropropan-2-yl)benzene (**1b**)

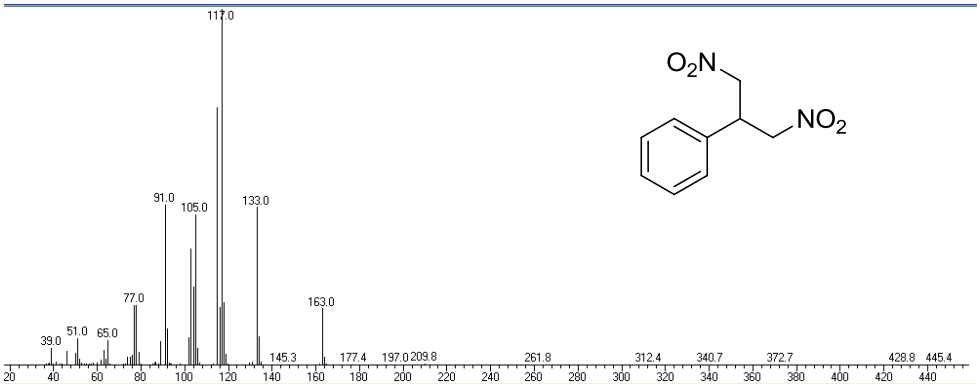

m/z calculated for $C_8H_9N_2O_4^{+\bullet}$ [$M^{+\bullet}$]: 210

❖ Dimethyl-2-(2-nitro-1-phenylethyl) malonate (**2**)

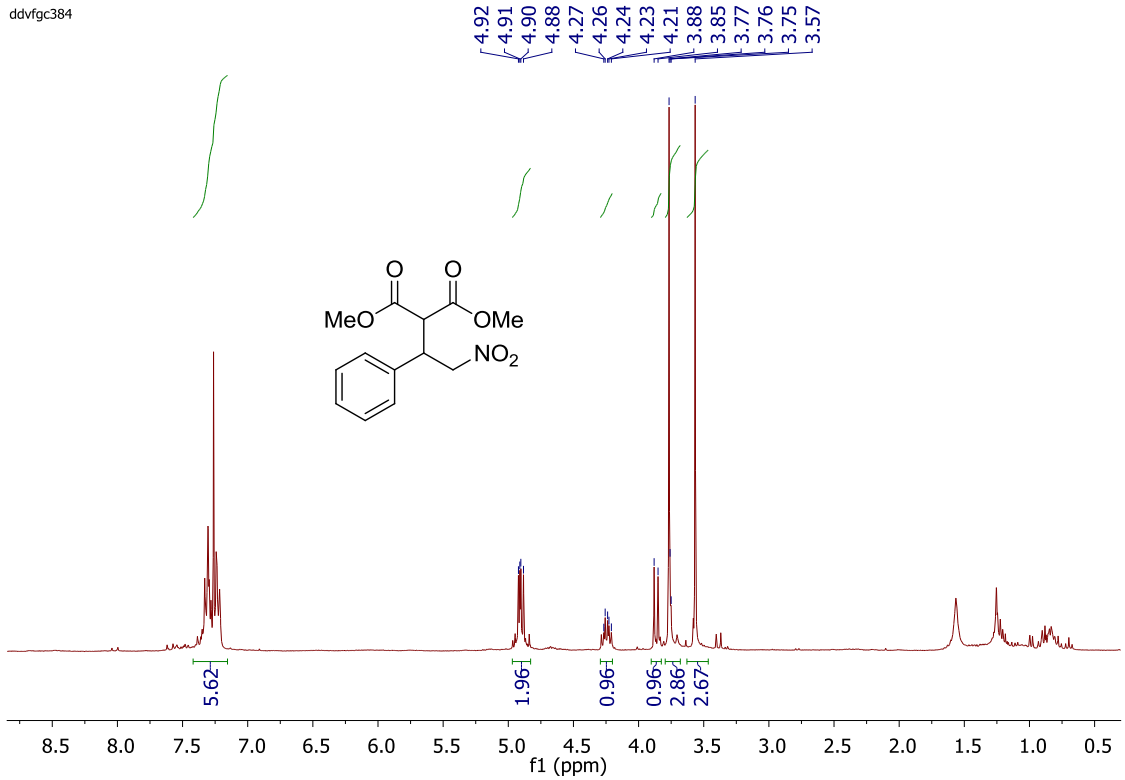

^{1}H NMR (300 MHz, $CDCl_3$) δ 7.44 – 7.13 (m, 5H), 5.00 – 4.78 (m, 2H), 4.25 (td, *J* = 8.7, 5.6 Hz, 1H), 3.86 (dd, *J* = 9.3, 4.6 Hz, 1H), 3.82 – 3.69 (m, 3H), 3.57 (d, *J* = 4.1 Hz, 3H).

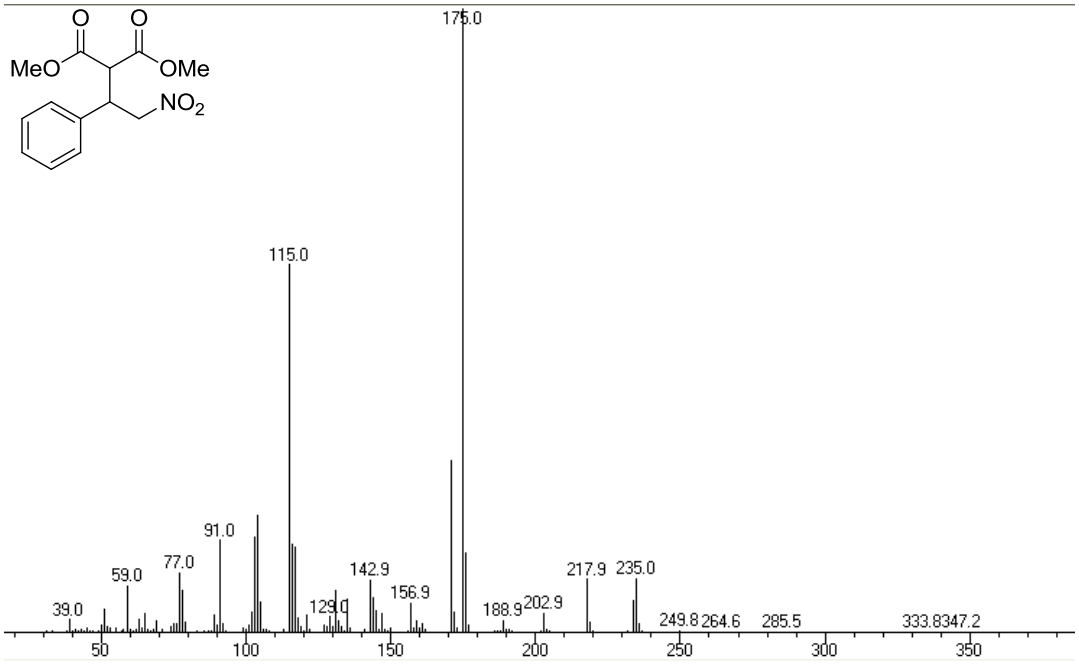

m/z calculated for $C_8H_7NO_2^{+\bullet}$ [$M^{+\bullet}$]: 235

❖ 3-(2-nitro-1-phenylethyl)-1H-indole (**3**)

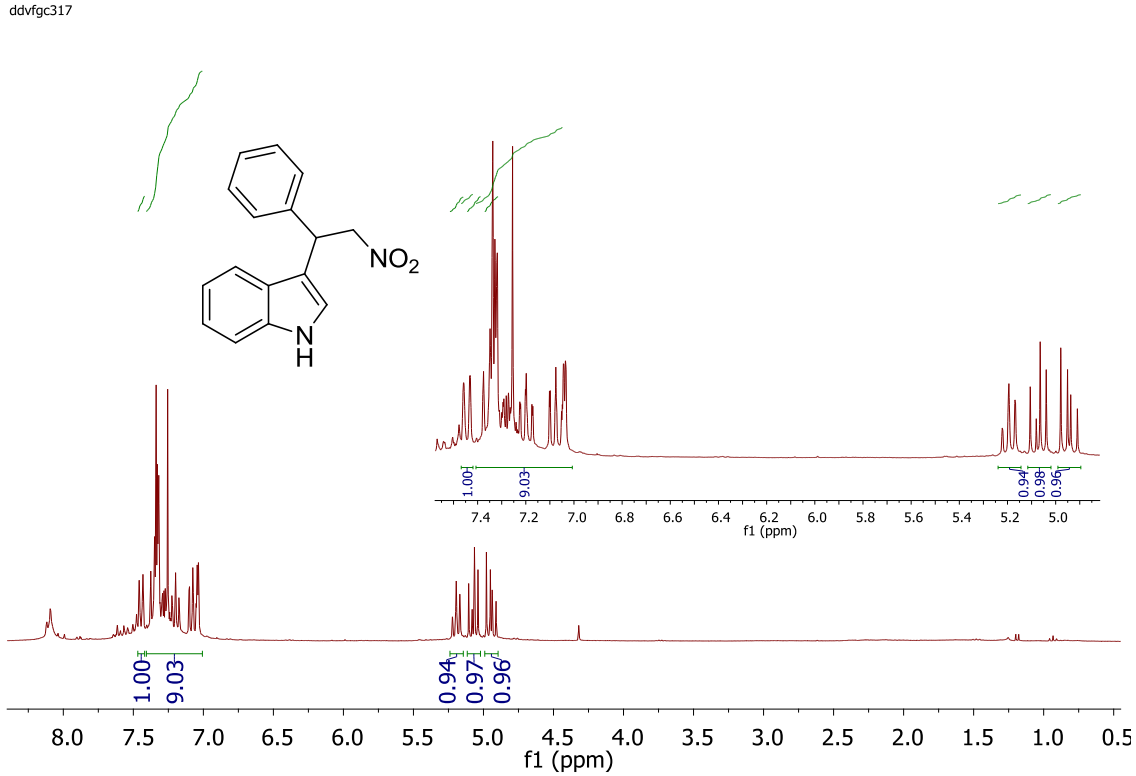

^{1}H NMR (300 MHz, $CDCl_3$) δ 7.44 (d, *J* = 8.0 Hz, 1H), 7.39 – 7.00 (m, 7H), 5.19 (t, *J* = 7.9 Hz, 1H), 5.06 (dt, *J* = 11.6, 5.8 Hz, 1H), 4.94 (dd, *J* = 12.4, 8.4 Hz, 1H).

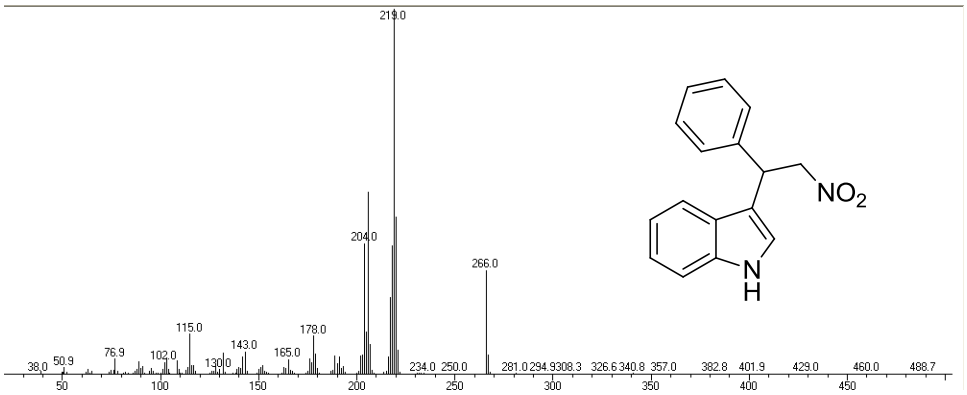

m/z calculated for $C_{16}H_{14}NO_2^{+\bullet}$ [$M^{+\bullet}$]: 266

References

(1) A. Maspero, S. Galli, N. Masciocchi, G. Palmisano, *Chem. Lett.* **2008**, *37*, 956.

(2) N. M. Padial, E. Quartapelle Procopio, C. Montoro, E. López, J. E. Oltra, V. Colombo, A. Maspero, N. Masciocchi, S. Galli, I. Senkovska, S. Kaskel, E. Barea, J. A. R. Navarro, *Angew. Chemie Int. Ed.* **2013**, *52*, 8290.

(3) E. Lopez-Maya, C. Montoro, V. Colombo, E. Barea, J. A. R. Navarro, *Adv. Funct. Mater.* **2014**, *24*, 6130.

(4) Y. Deng, A. D. Handoko, Y. Du, S. Xi, B. S. Yeo, *ACS Catal.* **2016**, 6, 2473−2481

(5) A. Cingolani, S. Galli, N. Masciocchi, L. Pandolfo, C. Pettinari, A. Sironi, *J. Am. Chem. Soc.* **2005**, *127*, 6144.

(6) N. Masciocchi, G. A. Ardizzoia, S. Brenna, G. LaMonica, A. Maspero, S. Galli, A. Sironi, *Inorg. Chem.* **2002**, *41*, 6080.

(7) Y. Li, X. Xie, J. Liu, M. Cai, J. Rogers, W. Shen, *Chem. Eng. J.* **2008**, *136*, 398–408.

(8) P. D. C. Dietzel, B. Panella, M. Hirscher, R. Blom, H. Fjellvag, *Chem. Commun.* **2006**, *9*, 959−961.